FINAL REPORT ON

AFOSR GRANT F49620-97-1-0356

FY 97 AASERT

1 MAY 1997 – 30 APRIL 1999

ICAM REPORT 99-09-01

20000728 076

DTIC QUALITY INSPECTED 4

OMB No. 0704-0188

Public reporting burden for this collection of information is estimated to average 1 hour per response, including the time for reviewing instructions, searching existing data sources, gathering and maintaining the data needed, and completing and reviewing the collection of information. Send comments regarding this burden estimate or any other aspect of this collection of information, including suggestions for reducing this burden, to Washington Headquarters Services, Directorate for Information Operations and Reports, 1215 Jefferson Davis Highway, Suite 1204, Arlington, VA 22202-4302, and to the Office of Management and Budget, Paperwork Reduction Project (0704-0188), Washington, DC 20503.

1. AGENCY USE ONLY (Leave blank)	2. REPORT DATE	3. REPORT TYPE AND DATES COVERED
	08/30/99	Final Report, 05/1/97 - 04/30/99

4. TITLE AND SUBTITLE

Adaptive Methods for Optimal Design (FY 97 AASERT)

5. FUNDING NUMBERS

(G) F49620-97-1-0356

6. AUTHOR(S)

J.A. Burns

AFRL-SR-BL-TR-00-

0333

7. PERFORMING ORGANIZATION NAME(S) AND ADDRESS(ES)

Interdisciplinary Center for Applied Mathematics
Wright House, West Campus Drive
Virginia Polytechnic Institute and State University
Blacksburg, Virginia 24061-0531

8. PERFORMING ORGANIZATION REPORT NUMBER

ICAM Report 99-09-01

9. SPONSORING/MONITORING AGENCY NAME(S) AND ADDRESS(ES)

Air Force Office of Scientific Research
Code NM
801 North Randolph Street
Arlington, VA 22203-1977

10. SPONSORING/MONITORING AGENCY REPORT NUMBER

11. SUPPLEMENTARY NOTES

12a. DISTRIBUTION/AVAILABILITY STATEMENT

Unlimited

Approved for public release,
distribution unlimited

12b. DISTRIBUTION CODE

13. ABSTRACT (Maximum 200 words)

This final technical report contains a summary and highlights of the research funded by AFOSR under Grant F49620-97-1-0356, titled "Adaptive Methods for Optimal Design (FY 97 AASERT)", for the period 1 May 1997 to 30 April 1999. This AASERT grant supported two graduate students to work on mathematical and computational methods for sensitivity analysis with application to shape optimization and optimal control of systems governed by partial differential equations. The focus of the project was the development of fast and accurate algorithms for sensitivity calculations and direct methods for computing functional gains for feedback control of thermal processes. We discovered that projection methods can greatly improved sensitivity accuracy in high Reynolds flows. We also observed faster and more robust convergence when projected gradients were employed. In addition, new numerical methods based on the method of mappings were constructed so that mesh gradients could be avoided. Our effort on feedback control generated new finite element schemes to numerically solve the Riccati partial differential equations that define feedback functional gains. In addition, Chandrasekhar partial differential equations were derived and used to construct new fast methods. These methods were applied to 2D problems. This report contains a summary of these results and a list of papers produced during this period.

14. SUBJECT TERMS

Optimal Design, Sensitivities, Feedback Control

15. NUMBER OF PAGES

40

16. PRICE CODE

17. SECURITY CLASSIFICATION OF REPORT	18. SECURITY CLASSIFICATION OF THIS PAGE	19. SECURITY CLASSIFICATION OF ABSTRACT	20. LIMITATION OF ABSTRACT
Unclassified	Unclassified	Unclassified	UL

FINAL TECHNICAL REPORT ON AFOSR GRANT

F49620-97-1-0356

Adaptive Methods for Optimal Design

(FY 97 AASERT)

THE AIR FORCE
CENTER FOR OPTIMAL DESIGN AND CONTROL

for the period

1 May 1997 - 30 April 1999

by

John A. Burns, Director
Air Force Center for Optimal Design and Control

Wright House / West Campus Drive
Virginia Polytechnic Institute & State University
Blacksburg, VA 24061- 0531

August 30, 1999

Prepared for the : **Air Force Office of Scientific Research**
Mathematical & Computer Sciences
801 North Randolph Street
Arlington, VA 22203-1977

Contents

Chapter 1

Introduction and Overview

This final report contains a summary of the activities supported under the Air Force AFOSR *AASERT* grant F49620-97-1-0356. This grant supported two graduate students, Lisa Stanley and Kevin Hulsing, to work with Professor John A. Burns (currently supported under AFOSR *PRET* Grant F49620-96-1-0329) on computational methods for optimal design and control of aerospace systems. In addition, the grant provided partial support for Major Dawn Stewart who completed her Ph.D at Virginia Tech. The research is based on our current work on mathematical and computational methods for sensitivity analysis and on new controller reduction methods for systems governed by partial differential equations. This work is fully described in the proposal "Sensitivity and Adjoint Methods for Design of Aerospace Systems" (this proposal resulted in the AFOSR *PRET* grant). The focus of this project is fundamental research in sensitivity based methods for optimal design and in computational methods for practical distributed parameter control. A major goal of this effort is to insure the transition of this work into Air Force and industrial applications. The research conducted by the *AASERT* students is motivated by the need to develop accurate solvers for sensitivity equations and to develop computational tools for controller reduction in 2D and 3D physics based models. The principal investigator is Dr. John A. Burns, Director of the Center for Optimal Design and Control and Hatcher Professor of Mathematics at Virginia Tech.

The *AASERT*students worked within the *PRET* Center at Virginia Tech. Research under the *PRET* Grant is conducted at six institutions: Virginia Tech, Cornell, AeroSoft, Beam Technologies, Boeing and Lockheed Martin. Frequent meetings of the team, exchange of visits, sharing of software, exchange of graduate students and postdoctoral researchers, industry-Air Force laboratory-university workshops and communication of results are coordinated by the Center.

The *PRET* Center offers an unparalleled potential for strengthening the educational and scientific infrastructure by training students and post-doctoral researchers in an interdisciplinary team approach to scientific and engineering research. The Center provides unique opportunities for theoretical, computational, and experimental research. Through the interactions with Air Force laboratories and industrial partners, students are exposed to real problems. The combined theoretical, computational, and experimental approach provides a meaningful interdisciplinary research experience.

The *AASERT* students played an integral role in the transition of research into industry and Air Force laboratories.

Chapter 2

Objectives

This *ASSERT* grant was designed to support the *PRET* program through the support of graduate students and their research. In addition to conducting basic research, these students played an integral role in the development of computational tools and in the transitioning of these tools to industry and Air Force laboratories.

2.1 Research Objectives

Although the *PRET* proposal contains several research objectives and the *AASERT* students are involved in several aspects of these projects, the *AASERT* students focused on two specific tasks with the following research objectives.

- **The development of fast and accurate computational methods for sensitivity analysis.** Sensitivity analysis plays a central role in optimal design as well as in the development of fast simulation algorithms. The goal of this effort was to improve the accuracy and efficiency in sensitivity computations by using adaptivity and smoothing methods. In addition, the method of mappings was investigated in order to improve accuracy.
- **The development of computational tools specifically for control design of distributed parameter systems.** The goal here is to develop practical computational tools for sensor/actuator placement and reduced order controller design. This goal was achieved by using distributed parameter theory, Chandrasekhar partial differential equations, and representations as a foundation for computational algorithms.

2.2 Educational Objectives, Interactions and Transitions

The educational goal of this *ASSERT* was to train interdisciplinary applied mathematicians, engineers and scientists to work on industrial problems of importance to the Air Force. This goal was met through interactions with *PRET* partners and the corresponding transition of research into these industries. In particular, we had the following specific educational objectives:

- **To develop an active program directed at educating interdisciplinary scientists and encouraging these graduates to work at Air Force facilities, laboratories and industry.** All of the students finished their Ph.D. degrees and are working on research important to the Air Force.
- **To transition research and computational tools into industry and Air Force laboratories.** We worked with our *PRET* partners to test new algorithms on design and control applications including (but not limited to) shape optimization and control design for flow management and heat transfer.

Chapter 3

Status of Effort

Considerable progress was made toward achieving the all of the proposed research objectives. The students developed new computational tools and began the construction of a mathematical framework that will allow for the analysis of these tools. This effort focused on the difficulties of producing practical design and control tools for complex 2D and 3D problems. This report contains a summary of new findings and accomplishments (Chapter 4) and the interactions/transitions (Chapter 7). However, the following items are particularly noteworthy.

Status of Effort

During this period, the two students supported under this grant produced 7 scientific papers, given more than 10 invited presentations and developed preliminary software packages for design and control. In addition, the students made considerable progress on three specific projects: adaptive finite element and projection methods for sensitivity computations, mapping techniques for sensitivity computations in elliptic systems, and numerical algorithms for computation of functional gains for feedback control of thermal processes.

Ms. Lisa Stanley, working with Major Dawn Stewart (USAF), developed a new algorithm for sensitivity calculations that is based on smoothing projections of spatial derivatives. They considered both local and global projections and tested the numerical methods on several boundary value problems. This work concentrated on projection error techniques for both state and sensitivity equations.

Major Stewart extended these methods to the Navier-Stokes equations and enhanced the performance of the basic algorithm by employing adaptive mesh generators to improve accuracy. Ms. Stanley investigated the method of mappings and used the continuous sensitivity method to produce accurate computational schemes. She showed that, if one first derives the sensitivity equation in the physical domain and then transforms both state and sensitivity equation to the computational domain, then mesh gradients are not needed and the accuracy of computed sensitivities can be controlled. This work also provides a theoretical framework for the rigorous analysis of the resulting algorithms.

Mr. Kevin Hulsing developed a fast new approach to the problem of computing functional gains that define optimal feedback controllers for spatially distributed systems. He derived Chandrasekhar partial differential equations for the gains and constructed numerical methods for solving these systems. He applied this method to 1D and 2D thermal control problems. This approach is based on direct solutions of Riccati and Chandrasekhar partial differential equations and allows the use of adaptive finite element methods (both p-refinement and h-refinement). In addition, he made use of "Nitsche" finite element techniques to enhance accuracy near the boundaries.

Chapter 4

Accomplishments and New Findings

This chapter contains a detailed summary of some of the research accomplishments and new findings, a brief description of research highlights and their significance to the field. In addition, we indicate the relevance of the research to potential Air Force applications and industrial technology challenges. In § 4.1 we present the highlights of Ms. Stanley's work on the use of transformations in sensitivity computations for elliptic systems. In § 4.2 we discuss Mr. Hulsing's work on numerical methods for computing functionsl gains for distributed processes. The following accomplishments are particularly important.

Accomplishment 1: Developed a Method of Mappings Method for Sensitivity Computations in Elliptic Boundary Value Problems

- **New Findings:** This algorithm is based on first deriving the sensitivity equations in the physical domain and then mapping both state and sensitivity equations to the computational domain. This approach allows for greater control of errors and eliminates the need to compute mesh gradients. In particular, these results show that errors in computing geometry sensitivities are important, but can be controlled by improving the boundary approximations alone.

- **Significance and Potential Applications:** Computing sensitivities in aerospace systems is fundamental to any design process. For large systems of differential equations, speed and accuracy of computation are essential. This work provides insight into the types of errors that must be controlled in order to achieve accuracy. In addition, the ability to compute sensitivity flow fields in a fraction of the time it takes to solve the basic equations, reduces design cycle times and allows the designer to evaluate the model as well as the design. These types of problems occur in several Air Force applications. The design and analysis of the COIL laser is just one of many such applications we are considering.

-

Accomplishment 2: Developed a Chandrasekhar PDE Approach for Computing Functional Gains for Feedback Control of Thermal Processes

- **New Findings:** This method is based on deriving a system of Chandrasekhar type partial differential equations that can be solved for the functional gains that define optimal feedback laws. The motivation is to develop new computational algorithms that can be applied to 2D and 3D distributed parameter systems. High order accurate schemes are used to solve the resulting system of partial differential equations. This method was applied to a 2D heat

transfer problem. Even when all other standard methods failed, the Chandrasekhar method converged to the gains. Therefore, this work established the feasibility of the approach for complex physisc based models.

- **Significance and Potential Applications:** In order to use functional gains for sensor/actuator placement and reduced order controller design, one first needs accurate approximations to these kernel functions. This new method not only improves accuracy, but also can provide this accuracy on coarse grids. In addition, the algorithm is highly parallelizable and allows for adaptivity. Thus, this type of method is more suitable for 2D and 3D control problems that occur in flow control and control of manufacturing processes.

4.1 Hybrid Transformation Methods for Sensitivity Computations

Sensitivity analysis is an important tool in engineering with applications ranging from optimal design to computational fluid dynamics. There are many algorithms available for computing sensitivities. These range from automatic differentiation techniques to variational methods. In this section we describe two variational methods for computing sensitivities. We use a 1D model problem as a platform for describing and comparing these methods. In particular, the regularity of the sensitivity equations obtained from each method is addressed. Numerical approximations to each sensitivity are calculated using finite element schemes, and numerical comparisons are presented.

4.1.1 Introduction

Accurate sensitivity calculations play an important role in the analysis and optimization of engineering systems. Sensitivities can be used to compute gradients in optimization-based design. In addition, they have been used to construct fast solvers for computational fluid dynamics. In this section, we focus on variational methods for computing state sensitivities. These schemes make use of sensitivity equation methods. However, there are a variety of ways to implement sensitivity equation methods, and these variations yield algorithms with different convergence properties. We consider two specific methods. The first is based on transforming the state equation to a fixed computational domain and then deriving its sensitivity equation. Once the state and sensitivity systems are solved, the solutions are mapped back to the physical domain. The second approach transforms both state and sensitivity equations, solves the transformed equations and maps these solutions back to the physical domain. There are benefits and drawbacks to each method. Indeed, it is not always obvious which scheme is best for a given problem. Many questions need to be addressed before a complete theory can be developed. In the discussion below, we will describe a simple 1D example in order to illustrate the methods and to motivate some of these questions. We begin with a description of the model problem. Each of the variational methods will be described in the context of the example, and numerical results will be presented. Finally, we will compare the performance of these methods and make some concluding remarks concerning future work.

4.1.2 Notation

Before describing the variational methods, we define the transformations used to move between the physical and the computational domains. Some notation regarding Sobolev spaces is also introduced. The "physical domain" for the model problem is the interval $(0, q)$, where q is a parameter with $q \in (1, 2)$. The computational domain is the unit interval $(0, 1)$. For $\alpha > 0$, let $\Omega_\alpha = (0, \alpha)$, and for each fixed $q \in (1, 2)$ define the transformation $T : \Omega_q \to \Omega_1$ by $T(x, q) = \frac{x}{q} = \xi$. Note that the function $M : \Omega_1 \to \Omega_q$ defined by $M(\xi) = \xi q = x$ is the inverse of T and is commonly referred to as the "mesh map".

Let $H^m(\Omega_1)$ denote the usual Sobolev space of "functions" whose partial derivatives, up to order m, are also square integrable. Let $L^2 = L^2(\Omega_1)$ with inner product defined by

$$\langle u, v \rangle = \int_0^1 u(\xi) v(\xi) d\xi$$

for all $u(\cdot), v(\cdot) \in L^2$. For this study, we need only to consider $V = H_0^1(\Omega_1) \subset H^1(\Omega_1)$, where V consists of functions in $H^1(\Omega_1)$ with zero trace. The dual space of V is given by $V^* = H^{-1}(\Omega_1)$. Finally, we need the bilinear form $a : V \times V \to \mathbb{R}$ by

$$a(\phi, \eta) = \int_0^1 \phi'(\xi) \eta'(\xi) d\xi \tag{4.1.1}$$

for all $\phi(\cdot), \eta(\cdot) \in V$.

4.1.3 A Model Problem

In this section, a 1D model problem is introduced. This example is convenient for numerical comparisons since both the state and the sensitivity equations have analytical solutions. The model problem is structured so that the physical domain is parameter dependent.

Let $1 < q < 2$, and consider the state equation given by the following elliptic boundary value problem

$$-w''(x) = f(x), \quad x \in (0, q) \tag{4.1.2}$$

with boundary conditions

$$w(0) = 0, \quad w(q) = 0. \tag{4.1.3}$$

Here $f : (0, +\infty) \to \mathbb{R}$ is the piecewise continuous function given by

$$f(x) = \begin{cases} 0, & 0 < x < 1 \\ -1, & 1 \leq x < +\infty. \end{cases} \tag{4.1.4}$$

The parameter q determines the length of the interval over which the state is defined. The goals are to solve (4.1.2)-(4.1.3) for the state, $w(x, q)$, for a given value of q and to determine the sensitivity of the state to small changes in the parameter. The sensitivity is denoted

$$s(x, q) \triangleq \partial_q w(x, q). \tag{4.1.5}$$

For this example, the state and sensitivity are given by

$$w(x, q) = \begin{cases} -\frac{(q-1)^2}{2q} x, & 0 < x < 1 \\ -\frac{(q-1)^2}{2q} x + \frac{1}{2}(x-1)^2, & 1 \leq x < q \end{cases} \tag{4.1.6}$$

and

$$s(x, q) = -\frac{(q^2 - 1)}{2q^2} x, \quad x \in (0, q), \tag{4.1.7}$$

respectively. However, we proceed to solve for both the state and the sensitivity numerically using each of the methods previously mentioned. Comparing the numerical calculations to (4.1.6)-(4.1.7) allows one to quantitatively measure the usefulness and accuracy of the methods. Note that for a fixed $\hat{q} > 1$, the function $x \to w(x, \hat{q})$ belongs to $H^2(0, \hat{q}) \cap H_0^1(0, \hat{q})$. However, $\partial_x^2 w(x, \hat{q})$ is discontinuous, while the sensitivity function, $x \to s(x, \hat{q})$ is C^∞. Having defined the relevant equations and unknowns, we will now use (4.1.2)-(4.1.3) to describe two methods for computing numerical approximations to $s(x, q)$.

4.1.4 Methods for Computing the Sensitivity

For many engineering applications, a typical approach to such problems is to begin by transforming the problem to a fixed "computational domain". This "computational domain" is often more regular in shape which simplifies grid generation and can improve the accuracy of numerical calculations. This technique is especially common for problems in computational fluid dynamics and for many problems involving moving boundaries such as shape optimization. The transformations can be performed at the infinite dimensional level as long as the mappings are isomorphisms and are sufficiently smooth in comparison to the regularity of the solution to the PDE in question. Both methods considered here make use of these transformations. It is important to note that in 2D and 3D problems, transforming can be a complex process. In particular, in addition to problems of regularity, it is important to consider accuracy loss. For example, transformations that produce coordinate systems that are orthogonal at boundaries are preferred. Otherwise, accuracy decreases as orthogonality declines. For the 1D example here, it is straightforward. Some of the difficulties that occur in 2D and 3D problems are not present in this case. In particular, this step often requires numerical approximations of the mapping and its spatial derivatives. More about this issue will be discussed in the conclusion.

4.1.5 Two Approaches for Sensitivity Calculation

Beginning with the state equation defined on the physical domain, one can implicitly differentiate the state (4.1.2)-(4.1.3) in order to obtain a sensitivity equation. At this stage, it is important to note that this differentiation is rather formal. In general, the partial derivatives $\partial_x^2 w(x,q)$ and $\partial_q w(x,q)$ need to be continuous in order to interchange the order of differentiation. In this case $\partial_x^2 w(x,q)$ is discontinuous, but one can verify by hand that the sensitivity $\partial_q w(x,q)$ satisfies the following differential equation

$$-s''(x) = 0, \quad 0 < x < q \tag{4.1.8}$$

with boundary conditions

$$s(0) = 0, \quad s(q) = -\partial_x w(q) = -\partial_x w(x)\Big|_{x=q}. \tag{4.1.9}$$

System (4.1.8)-(4.1.9) is called the sensitivity equation. The boundary conditions should be derived with care as the right endpoint of the domain $(0,q)$ depends explicitly on the parameter q.

Once the sensitivity equation has been derived on the physical domain, the transformations in Section 4.1.2 are used to define the "transformed" functions. For $\xi \in \Omega_1$ and $q \in (1,2)$, define

$$\begin{aligned} \hat{w}(\xi,q) =& w(M(\xi,q),q) = w(x,q), \\ \hat{s}(\xi,q) =& s(M(\xi,q),q) = s(x,q) \end{aligned} \tag{4.1.10}$$

and

$$\hat{f}(\xi,q) = f(M(\xi,q),q) = f(x). \tag{4.1.11}$$

Once transformed, the original forcing function f becomes

$$\hat{f}(\xi,q) = \begin{cases} 0, & 0 < \xi < \frac{1}{q} \\ -1, & \frac{1}{q} \le \xi < 1 \end{cases} \tag{4.1.12}$$

and now depends explicitly on the parameter q. Using the above definitions and the chain rule, the spatial derivatives of the original functions and those of the transformed functions are related by

$$\begin{aligned} \partial_x w(x,q) &= \partial_\xi \hat{w}(T(x,q),q) \cdot \partial_x T(x,q) \\ &= \partial_\xi \hat{w}(\xi,q) \cdot \frac{1}{q} \end{aligned} \tag{4.1.13}$$

and

$$\begin{aligned} \partial_x^2 w(x,q) &= \partial_\xi^2 \hat{w}(T(x,q),q) \cdot [\partial_x T(x,q)]^2 + \\ &\qquad \partial_\xi \hat{w}(T(x,q),q) \cdot \partial_x^2 T(x,q) \\ &= \partial^2{}_\xi \hat{w}(\xi,q) \cdot \frac{1}{q^2}. \end{aligned} \tag{4.1.14}$$

These identities are used to derive transformed boundary value problems for both the transformed state and the transformed sensitivity in (4.1.10). The transformed state equation is defined by the differential equation

$$-\hat{w}''(\xi) = q^2 \hat{f}(\xi,q), \quad \xi \in (0,1), \tag{4.1.15}$$

with boundary conditions

$$\hat{w}(0) = 0, \quad \hat{w}(1) = 0. \tag{4.1.16}$$

Likewise, the transformed sensitivity equation is given by the differential equation

$$-\hat{s}''(\xi) = 0, \quad \xi \in (0,1), \tag{4.1.17}$$

with boundary conditions

$$\hat{s}(0) = 0, \quad \hat{s}(1) = -\left(\frac{1}{q}\right) \cdot \partial_\xi \hat{w}(1) = -\left(\frac{1}{q}\right) \cdot \partial_\xi \hat{w}(\xi)\Big|_{\xi=1}. \tag{4.1.18}$$

Using (4.1.6) and (4.1.7), the solutions to the transformed state and sensitivity equations are given by

$$\hat{w}(\xi, q) = \begin{cases} -\frac{(q-1)^2}{2}\xi, & 0 < \xi < \frac{1}{q} \\ -\frac{(q-1)^2}{2}\xi + \frac{(\xi q-1)^2}{2}, & \frac{1}{q} < \xi < 1 \end{cases} \tag{4.1.19}$$

and

$$\hat{s}(\xi, q) = -\frac{(q^2-1)}{2q}\xi, \quad 0 < \xi < 1, \tag{4.1.20}$$

respectively.

Before describing the variational formulations and the discretization, we will discuss an alternate approach. The process we outline in the following paragraphs varies from the one previously described in the order in which the sensitivity equation is derived and the transformations are performed.

A second approach to the computation of the sensitivity is similar in spirit to the *Semi-Analytical* method (SAM). This technique is often used in the engineering community. Roughly speaking, the SAM begins by first transforming the state equation to the computational domain. The second step is to discretize the state equation, thereby producing an algebraic system. This discrete equation is then differentiated to obtain a discrete sensitivity equation which is solved using special techniques. An abstract version of this method (A-SAM) may be constructed by deriving a sensitivity equation after transforming but before discretizing the state equation. In particular, the infinite dimensional transformed state equation is "differentiated" in order to obtain an equation for the sensitivity of the transformed state. We now present the details of this approach.

On the computational domain, Ω_1, define the sensitivity of the transformed state by $p(\xi, q) = \partial_q \hat{w}(\xi, q)$. In order to derive a system for $p(\xi, q)$, the transformed state equation (4.1.15)-(4.1.16) is "differentiated" with respect to q. This requires that the function $\hat{f}(\xi, q)$ be "differentiated" with respect to q as well. As before, formal differentiation yields the boundary value problem

$$-\partial_\xi^2 p(\xi, q) = g(\xi, q), \tag{4.1.21}$$

$$p(0) = 0, \quad p(1) = 0, \tag{4.1.22}$$

where $g(\xi, q) \triangleq 2q\hat{f}(\xi, q) + q^2 \partial_q \hat{f}(\xi, q)$ belongs to V^*. In particular,

$$g(\xi, q) = 2q\hat{f}(\xi, q) - \delta_{\frac{1}{q}}(\xi), \tag{4.1.23}$$

where $\delta_{\frac{1}{q}}(\xi)$ is the delta function with mass at $\frac{1}{q}$. Since the linear elliptic problem (4.1.21)-(4.1.22) does not have $H^2(\Omega_1)$ solutions, the system must be considered in the weak sense. We use this system to derive a weak formulation in Section 4.1.6.

For this example, $p(\xi, q)$ can be calculated directly from (4.1.19) to obtain

$$\partial_q \hat{w}(\xi, q) = p(\xi, q) = \begin{cases} -(q-1)\xi, & 0 < \xi < \frac{1}{q} \\ -(q-1)\xi + (\xi q - 1)\xi, & \frac{1}{q} < \xi < 1. \end{cases} \tag{4.1.24}$$

Clearly, $\widehat{\partial_q w(x,q)} = \hat{s}(\xi,q) \neq p(\xi,q)$. In particular, we observe that the sensitivity of the transformed state, $p(\xi,q)$, is less smooth than the transformed sensitivity $\hat{s}(\xi,q)$ in (4.1.20). Furthermore, the relationship between the transformed sensitivity and the sensitivity of the transformed state can be derived using (4.1.13)-(4.1.14) and the chain rule. Beginning with the definition of the sensitivity of the transformed state, it follows that

$$\begin{aligned} p(\xi,q) &= \partial_q \hat{w}(\xi,q) \\ &= \partial_q w(M(\xi,q),q) \\ &= \partial_q w(M(\xi,q),q) + \partial_x w(M(\xi,q),q)\,[\partial_q M(\xi,q)] \\ &= s(M(\xi,q),q) + \partial_x w(x,q)\,[\partial_q M(\xi,q)] \\ &= \hat{s}(\xi,q) + [\partial_x T(x,q)]\,\partial_\xi \hat{w}(\xi,q)\,[\partial_q M(\xi,q)] \\ &= \hat{s}(\xi,q) + [\partial_\xi M(\xi,q)]^{-1}\,\partial_\xi \hat{w}(\xi,q)\,[\partial_q M(\xi,q)]\,. \end{aligned}$$

The relationship between $s(x,q)$ and $p(\xi,q)$ can be obtained by using (4.1.10) and the definition of the transformation T. Direct computation yields

$$s(x,q) = p(\frac{x}{q},q) - \partial_\xi \hat{w}(\frac{x}{q},q)\left[\partial_\xi M(\frac{x}{q},q)\right]^{-1}\left[\partial_q M(\frac{x}{q},q)\right]. \tag{4.1.25}$$

Observe the appearance of the "mesh derivative", $\partial_q M(\xi,q)$, and the spatial derivative of $\hat{w}(\xi,q)$ in this equation. In order to calculate $s(x,q)$ using this (A-SAM) approach, one needs to compute not only the sensitivity of the transformed state but also the spatial derivative of the transformed state and the mesh derivative. For this example, $\partial_q M(\xi,q)$ is easily accessible. However, for 2D and 3D problems, these maps are constructed using numerical algorithms, and obtaining derivatives of the maps can be very difficult. Using the preceding definitions, we define two methods for computing the sensitivity $s(x,q)$.

Hybrid-Sensitivity Equation Method (H-SEM)

Step 1. Solve the transformed state equation (4.1.15)-(4.1.16) for $\hat{w}(\xi,q)$.

Step 2. Solve the transformed sensitivity equation (4.1.17)-(4.1.18) for $\hat{s}(\xi,q)$.

Step 3. Map $\hat{s}(\xi,q)$ back to the physical domain to obtain the sensitivity by

$$s(x,q) = \hat{s}(T(x,q),q).$$

Abstract-Semi Analytical Method (A-SAM)

Step 1. Solve the transformed state equation (4.1.15)-(4.1.16) for $\hat{w}(\xi,q)$.

Step 2. Solve (4.1.21)-(4.1.22) for the sensitivity of the transformed state $p(\xi,q)$.

Step 3. Map $p(\xi,q)$ back to the physical domain to obtain the sensitivity using

$$s(x,q) = p(\frac{x}{q},q) - \partial_\xi \hat{w}(\frac{x}{q},q)\left[\partial_\xi M(\frac{x}{q},q)\right]^{-1}\left[\partial_q M(\frac{x}{q},q)\right].$$

Differences in the regularity of the sensitivity equations have already been noted. We want to examine the effect of these differences on numerical approximations of the sensitivities. The following sections explore some computational issues that are relevant to each method. Variational formulations are described, and a brief section outlining the discretization is presented.

4.1.6 Variational Formulations

We begin by considering the transformed state equation in (4.1.15)-(4.1.16). Multiplying by an arbitrary function $\eta \in V$ and integrating by parts, we have the following integral equation

$$\int_0^1 \hat{w}'(\xi)\eta'(\xi)d\xi = q^2 \int_0^1 \hat{f}(\xi)\eta(\xi)d\xi \qquad \forall\, \eta \in V. \tag{4.1.26}$$

This equation, along with the bilinear form and L^2-inner product defined in Section 4.1.2, produces the variational form of (4.1.15)-(4.1.16). In particular, (4.1.15)-(4.1.16) is equivalent to the following variational equation. Find $\hat{w}(\cdot) \in V$ such that

$$a(\hat{w}, \eta) = q^2 \langle \hat{f}(\cdot, q), \eta(\cdot) \rangle \tag{4.1.27}$$

for all $\eta(\cdot) \in V$.

We now turn to the transformed sensitivity equation. Note that the boundary conditions (4.1.18) are nonhomogeneous. In order to simplify notation, we denote the right boundary condition of (4.1.18) by $\gamma = \frac{-1}{q}\partial_\xi \hat{w}(1)$. If $s^*(\xi, q)$ is defined by the function

$$s^*(\xi, q) \triangleq \gamma\xi, \tag{4.1.28}$$

then $s^*(\xi, q) \in H^1(\Omega_1)$ and $s^*(\xi, q)$ satisfies the boundary conditions $s^*(0) = 0$ and $s^*(1) = \gamma$. It follows that $v(\xi, q) = \hat{s}(\xi, q) - s^*(\xi, q)$ belongs to V and solves the differential equation

$$-v''(\xi, q) = 0 \tag{4.1.29}$$

with homogeneous Dirichlet boundary conditions

$$v(0, q) = 0 \quad v(1, q) = 0. \tag{4.1.30}$$

The corresponding variational equation is defined in V. Find $v(\cdot) \in V$ such that

$$a(v, \eta) = 0 \tag{4.1.31}$$

for all $\eta(\cdot) \in V$. Once $v(\xi, q)$ is computed, the transformed sensitivity $\hat{s}(\xi, q)$ is recovered using the relationship $\hat{s}(\xi, q) = v(\xi, q) + s^*(\xi, q)$.

We now derive the variational problem involving the sensitivity of the transformed state, $p(\xi, q)$. As noted in Section 4.1.5, the system in (4.1.21)-(4.1.22) must be interpreted in the space V^*. That is, the following equation holds

$$\begin{aligned} \int_0^1 p'(\xi)\eta'(\xi)d\xi &= 2q \int_0^1 \hat{f}(\xi, q)\eta(\xi)d\xi - \int_0^1 \delta_{\frac{1}{q}}(\xi)\eta(\xi)d\xi \\ &= 2q \int_0^1 \hat{f}(\xi, q)\eta(\xi)d\xi - \eta(\frac{1}{q}) \end{aligned} \tag{4.1.32}$$

for all $\eta(\cdot) \in V$. Define the linear functional $l_q \in V^*$ by

$$l_q(\eta) = 2q\langle \hat{f}, \eta \rangle - \delta_{\frac{1}{q}}(\eta) \tag{4.1.33}$$

for all $\eta(\cdot) \in V$. It follows that equation (4.1.32) is equivalent to the following variational problem. Find $p(\cdot) \in V$ so that

$$a(p, \eta) = l_q(\eta) \tag{4.1.34}$$

for all $\eta(\cdot) \in V$.

Before turning to numerical issues, we note that this example falls within a general framework that provides the basic existence, uniqueness and differentiability of the transformed state equation. Observe that the variational problem (4.1.27) has the form

$$\mathcal{A}\hat{w} = \mathbf{F}(q) \quad \text{in } V^*, \tag{4.1.35}$$

where $\mathcal{A}\colon V \to V^*$ and $\mathbf{F}\colon \mathbb{R} \to V^*$ are defined by

$$[\mathcal{A}u](v) = a(u,v) \qquad \forall\, v \in V \tag{4.1.36}$$

and

$$[\mathbf{F}(q)](v) = q^2\langle \hat{f}(\cdot,q), v(\cdot)\rangle \qquad \forall\, v \in V, \tag{4.1.37}$$

respectively. If one defines the function $\mathbf{G}\colon V \times \mathbb{R} \to V^*$ by

$$\mathbf{G}(\hat{w},q) = \mathcal{A}\hat{w} - \mathbf{F}(q), \tag{4.1.38}$$

then the following result provides the theoretical foundation for the numerical methods presented below.

Theorem 4.1.1. *If $q \in (1,2)$, then $\mathbf{G}(\hat{w},q) = 0$ has a unique solution $\hat{w} = \hat{w}(\cdot,q)$. Moreover, $p(\cdot,q) = \partial_q \hat{w}(\cdot,q)$ exists and is the unique solution to the sensitivity equation (in V^*)*

$$\mathcal{A}p - \partial_q \mathbf{F}(q) = 0. \tag{4.1.39}$$

The proof of Theorem 4.1.1 follows easily from the implicit function theorem. In particular, one can show that the strong Fréchet derivatives $\partial_{\hat{w}}\mathbf{G}(\hat{w},q)$ and $\partial_q \mathbf{G}(\hat{w},q)$ exist and are given by

$$\partial_{\hat{w}}\mathbf{G}(\hat{w},q) = \mathcal{A}, \tag{4.1.40}$$

and

$$\partial_q \mathbf{G}(\hat{w},q) = -\partial_q \mathbf{F}(q) = -l_q(\cdot), \tag{4.1.41}$$

where $l_q(\cdot)$ is defined by (4.1.33). Observe that the sensitivity equation (4.1.39) is equivalent to the variational problem (4.1.34).

Although the framework defined by (4.1.35) - (4.1.39) is suitable for many elliptic problems, it is not sufficient for more general shape sensitivity problems. For example, the classical elliptic interface problem requires a more general theory. We now move to the numerical approximation of the solutions to the variational problems. The following section describes the appropriate finite element spaces for approximating the transformed state, $\hat{w}(\xi,q)$, the transformed sensitivity, $\hat{s}(\xi,q)$ and the sensitivity of the transformed state, $p(\xi,q)$.

Discretization

For the finite element approximation of the variational equations, we begin by constructing the grid. Note that the function $\hat{f}(\xi,q)$ is discontinuous at the point $\xi = \frac{1}{q}$ in the computational domain. Hence, a grid point of the mesh is placed at that point. We partition the domain Ω_1 into subintervals (ξ_j, ξ_{j+1}) where $0 = \xi_0 < \xi_1 < \cdots < \xi_k = \frac{1}{q} < \cdots < \xi_N < \xi_{N+1} = 1$. We choose the finite dimensional subspace of V to be the space spanned by N piecewise linear basis functions denoted

$$V^N = \{\psi(\cdot) \in V : \psi(\xi) = \sum_{j=1}^{N} c_j h_j(\xi)\}, \tag{4.1.42}$$

where $h_j(\xi)$ is the standard continuous piecewise linear basis function.

For the computations presented in the following sections, we use the partition of Ω_1 developed above for both state and sensitivity approximations. Hence, the mesh (ξ_j, ξ_{j+1}), for $j = 0, 1, \ldots N$ is used to calculate approximations to $\hat{w}(\xi, q)$, $v(\xi)$ and $p(\xi, q)$. The function $v(\xi)$ is approximated in the same manner as the transformed state. In particular, we let

$$\hat{w}^N(\xi) = \sum_{j=1}^{N} \alpha_j h_j(\xi), \tag{4.1.43}$$

$$p^N(\xi, q) = \sum_{j=1}^{N} \tau_j h_j(\xi) \tag{4.1.44}$$

and

$$v^N(\xi) = \sum_{j=1}^{N} \beta_j h_j(\xi) \tag{4.1.45}$$

be finite element approximations of $\hat{w}(\xi, q)$, $p(\xi, q)$ and $v(\xi)$, respectively. Once $v^N(\xi)$ has been obtained, we compute the approximation of the transformed sensitivity using

$$\hat{s}_H^N(\xi, q) = v^N(\xi) + \gamma^N \xi, \tag{4.1.46}$$

where γ^N is the approximation to $\gamma = \frac{-1}{q}\partial_\xi \hat{w}(1, q)$ given by

$$\gamma^N = \frac{-1}{q}\partial_\xi \hat{w}^N(1, q). \tag{4.1.47}$$

Note that the subscript notation used on $\hat{s}_H^N(\xi, q)$ refers to the use of the H-SEM approach for the sensitivity calculation.

Remark: The use of γ^N for γ introduces error into $\hat{s}_H^N(\xi, q)$ that is independent of the error in $v^N(\xi, q)$. However, this error significantly affects the accuracy of $\hat{s}(\xi, q)$, and eventually, that of $s(x, q)$. It is also noteworthy that even though the weak form of (4.1.34) does not require spatial information about $\hat{w}(\xi)$, the spatial derivative $\partial_\xi \hat{w}(\xi)$ is required to reconstruct $s(x, q)$ through (4.1.25). These issues play an important role in the numerical results presented in Section 4.1.7.

4.1.7 Numerical Results

In this section, we present numerical approximations to $w(x, q)$ and $s(x, q)$ using the methods described in the previous section. We compare numerical approximations of $s(x, q)$ that result from implementing each of the methods discussed in Section 4.1.5. In particular, we compare results obtained using H-SEM with those of the A-SAM.

State Approximations

All computations presented use the same grids for both sensitivity approximations. It is important to recall that a node is placed at $\xi = \frac{1}{q}$. Figure 4.1.1 shows the finite element approximations to $\hat{w}^N(\xi, 1.5)$ for various values of N. These approximations converge rapidly. Similar behavior is observed over a range of parameter values. The corresponding approximations to $w^N(x, 1.5)$, obtained by transforming the finite element approximation, $\hat{w}^N(\xi, q)$, back to the physical domain, are shown in Figure 4.1.2. Comparing Figures 4.1.1 and 4.1.2, one can see that convergence of the approximations is preserved under the transformation T.

Figure 4.1.3 shows the H^1-error in $w(x, q)$ for values of q between 1.1 to 1.9. The values of N range from 3 to 33 and are indicated in the legend. Note that the rate of convergence is better for $q \to 1$ as the quadratic term (see (4.1.19)) in the transformed state becomes less dominant.

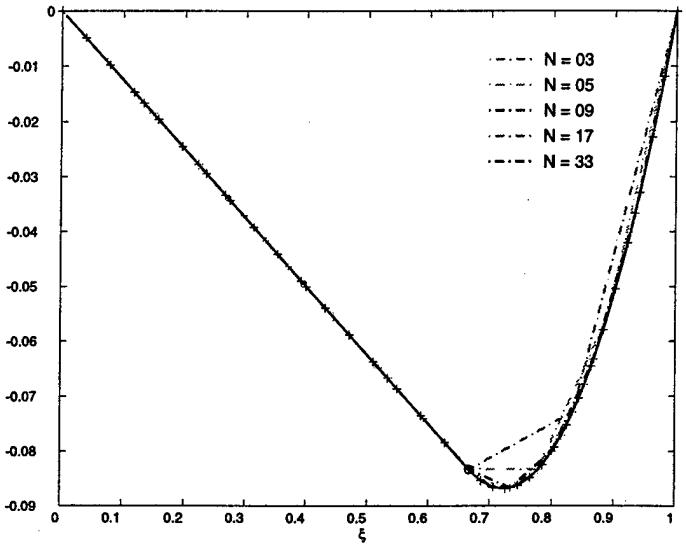

Figure 4.1.1: Finite Element Approximations to $\hat{w}(\xi, 1.5)$

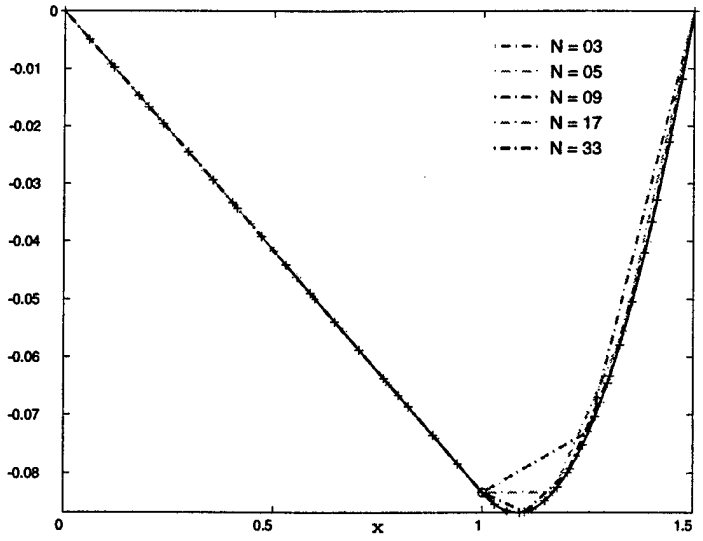

Figure 4.1.2: Approximations to $w(x, 1.5)$

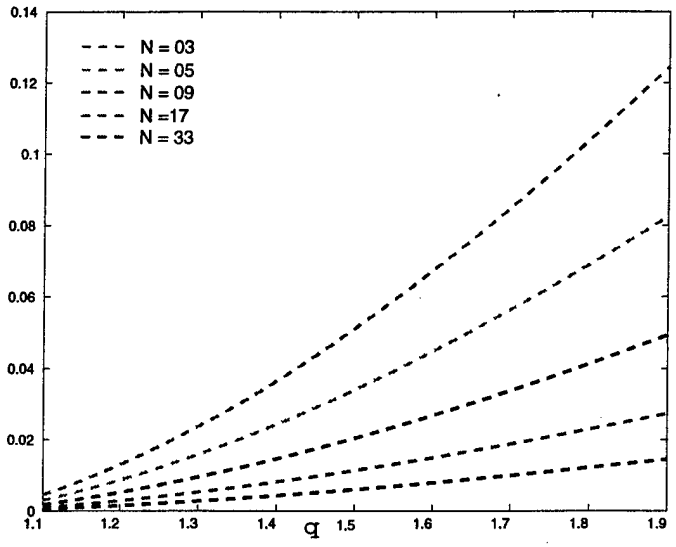

Figure 4.1.3: H^1-Error of $w^N(x)$ for q ranging from 1.1 to 1.9

Hybrid Sensitivity Equation Method

In this section, we present sensitivity calculations obtained by applying the H-SEM algorithm. Figure 4.1.4 shows the convergence of the finite element approximations to $\hat{s}(\xi, 1.5)$. Observe that the entire error results from the approximation of $\gamma = \frac{-1}{q}\partial_\xi \hat{w}(1,q)$ by $\gamma^N = \frac{-1}{q}\partial_\xi \hat{w}^N(1,q)$. Since the transformation T is smooth, the only error in $s_H^N(x, 1.5)$ is due to this approximation. Figure 4.1.5 shows the convergence of $s_H^N(x, 1.5)$ to $s(x, 1.5)$.

Recall that $\hat{w}^N(\xi)$ is a piecewise linear approximation. Thus, the finite element spatial derivative is a piecewise constant function. This function is used to approximate the spatial derivative at the right boundary point $\xi = 1$. Figure 4.1.6 shows a piecewise constant approximation used to obtain an approximate boundary condition γ^N. Hence, the error in $\partial_\xi \hat{w}(1)$ results in sensitivity errors that can be attributed to the poor approximation of this boundary condition. There are techniques which can be used to obtain better approximations to the spatial derivative along the boundary. Higher order elements can be used in the transformed state calculation, but this can be costly for 2D and 3D problems. As an alternative, projection techniques have been developed to enhance the accuracy of the spatial derivative for nominal expense. We move to the A-SAM.

Abstract *Semi-Analytical* Method

We turn our attention to numerical results obtained by using the A-SAM algorithm for sensitivity calculations. First, note that $s_A^N(x)$ is constructed from $p^N(\xi, q)$ and $\partial_x \hat{w}^N(\xi)$ using the relationship.

$$s_A^N(x,q) = p^N(\frac{x}{q}, q) - \left(\frac{x}{q^2}\right)\partial_\xi \hat{w}^N(\frac{x}{q}, q). \tag{4.1.48}$$

Note that we use the subscript A for the sensitivity approximation obtained using the A-SAM approach. The finite element approximations to $p(\xi, 1.5)$ are shown in Figure 4.1.7 for various values of N. Since the sensitivity equations are linear, the approximations $p^N(\xi, 1.5)$ converge as expected. When constructing $s_A^N(x, 1.5)$ from (4.1.48), the piecewise constant approximation of $\partial_x \hat{w}^N(\xi)$ produces discontinuities in $s_A^N(x)$ as shown in Figure (4.1.8). These discontinuities occur at points of the physical domain which correspond to mesh nodes of the computational domain lying in the interval $[\frac{1}{q}, 1)$. Note that the expressions for the mesh derivatives in (4.1.48) are "hard-wired", continuous functions, and the finite element approximations to $p(\xi, q)$ are continuous. It follows that

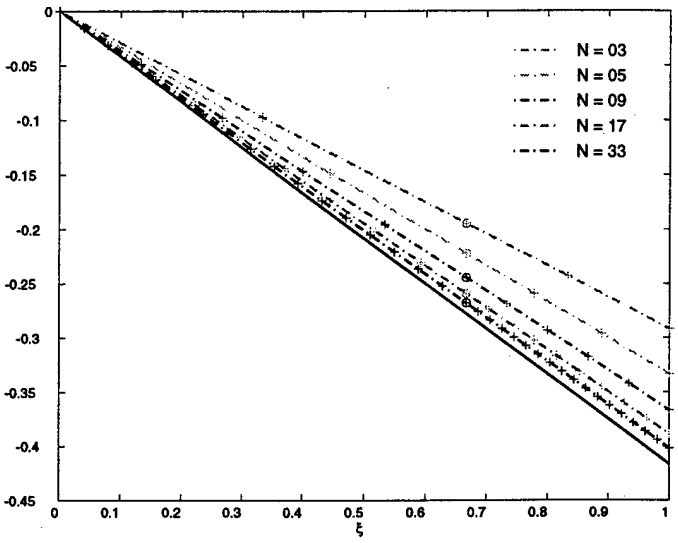

Figure 4.1.4: Finite Element Approximations to $\hat{s}(x, 1.5)$

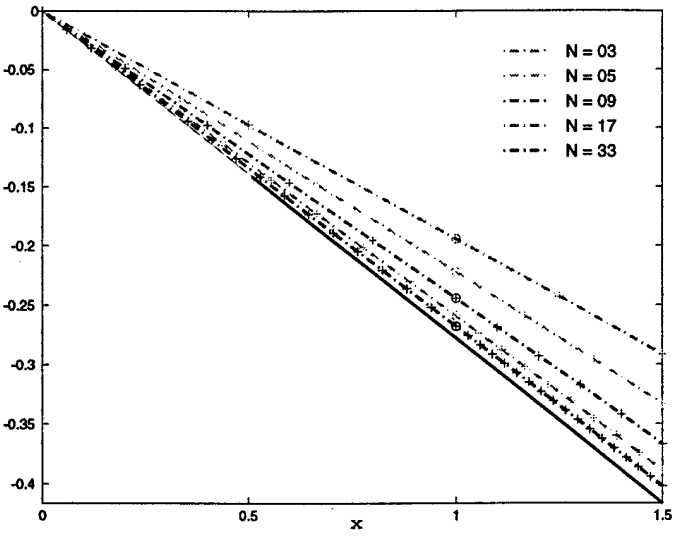

Figure 4.1.5: H-SEM Approximations to $s(x, 1.5)$

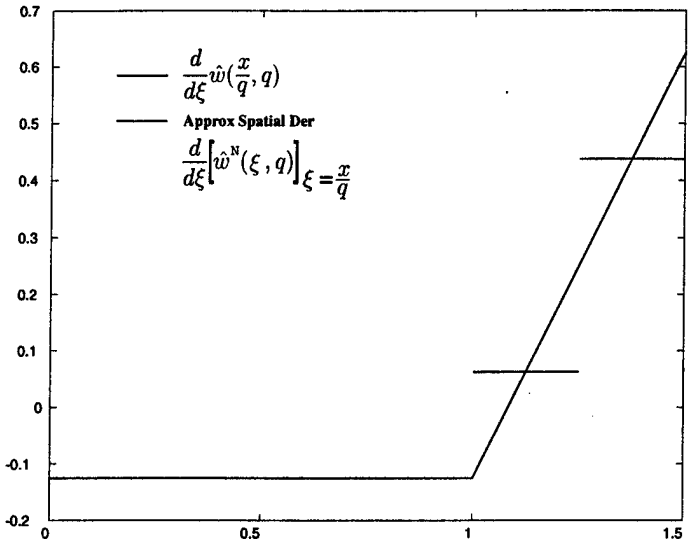

Figure 4.1.6: Approximation of $\partial_x \hat{w}(\xi, 1.5)$ with $N = 3$

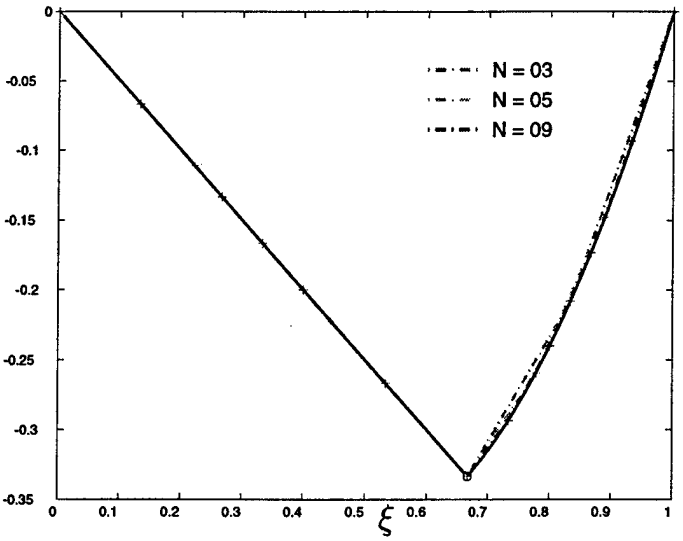

Figure 4.1.7: Finite Element Approximations to $p(\xi, 1.5)$

$\|s(x,q) - s_A^N(x,q)\|_{L^2} \to 0$ as $N \to \infty$. However, one does not get convergence in the energy (H_0^1) norm since $\partial_x s_A^N(x,q)$ is not in V.

4.1.8 Conclusion

Each of the methods described above present computational challenges. The Hybrid SEM requires gradient information along the boundary of the computational domain. Even in the 1D example, this information becomes critical to accurate sensitivity calculations. Approximating gradients along the boundary only gets more challenging in 2D and 3D problems. However, the Abstract SAM requires accurate gradient information within the computational domain. This example clearly illustrates the serious contamination of sensitivity approximations that can occur if the approximate gradients are inaccurate or are not sufficiently smooth. Moreover, the issue of calculating derivatives of mesh maps is not addressed in this 1D example. Those were analytically computed and "hard-wired" into

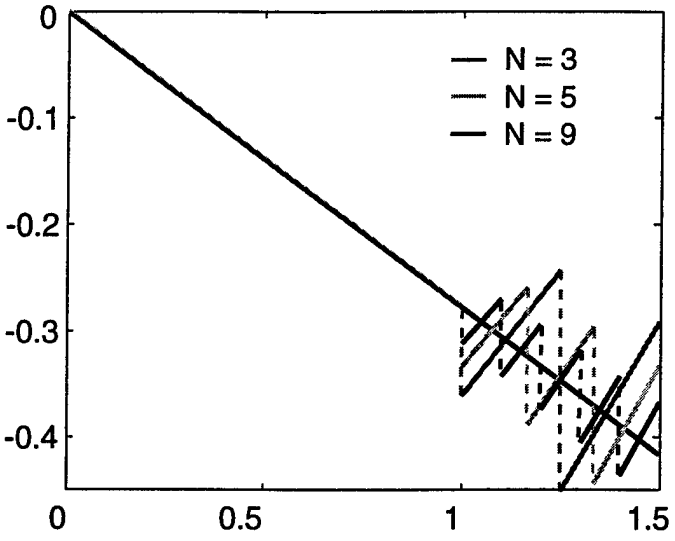

Figure 4.1.8: A-SAM Approximations to $s(x, 1.5)$

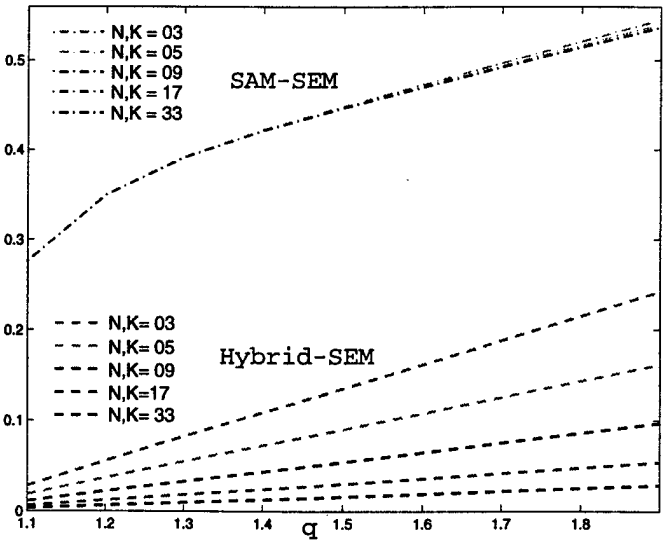

Figure 4.1.9: H^1 Errors for Sensitivity Calculations

the computations. In practical problems, calculating these derivatives can be an extremely difficult task as well as a source of computational error. Both methods require accurate gradient information from the transformed state. In the case of the Hybrid method, this is the only major stumbling block to obtaining reliable sensitivity calculations. In contrast, accurate gradient information may not be sufficient to obtain good sensitivity approximations using the Abstract SAM method as the need for accurate mesh derivatives may overshadow the entire process.

4.2 Fast Algorithms for Computing Functional Gains

Functional gains are kernels of feedback operators that result from distributed parameter control problems defined by partial and functional differential equations. These gains offer insight into issues such as sensor/actuator placement and controller reduction. To be practical, one must be able to compute these kernels for a wide variety of partial differential equations in 2 and 3 spatial dimensions. Standard "approximate-then-design" approaches have been very useful for small 1D problems. However, in 2D and 3D problems, the size of the approximating systems limits this method as a practical computational tool. Therefore, alternative methods are needed.

As a first step in the direction we have investigated the possibility of using "direct" approximations of Riccati and Chandrasekhar partial differential equations that define the kernels. In this short note we illustrate this idea by using finite element schemes to solve these partial differential equations. One important observation about this direct approach is that it allows for the possibility of using parallel and adaptive computational tools. In addition, we show that modifications of "standard" finite element schemes can often improve the speed and accuracy of the old indirect schemes. The goal of the current note is to illustrate the basic ideas and provide some introduction to the theoretical and computational issues that arise in this problem area.

4.2.1 Dirichlet Boundary Control

The one-dimensional heat equation with Dirichlet boundary controls is defined by the initial boundary value problem:

$$\left.\begin{aligned} z_t(t,x) &= \epsilon z_{xx}(t,x), \\ z(t,0) = u_0(t), \qquad & z(t,1) = u_1(t), \\ z(0,x) &= z_0(x), \end{aligned}\right\} \tag{4.2.49}$$

where ϵ is the thermal diffusivity of the material.

In order to take advantage of distributed parameter control theory, we first formulate the boundary value problem (4.2.49) as an abstract state space model. In particular, we write the problem as a system of the form

$$\left.\begin{aligned} \dot{z}(t) &= \tilde{A}z(t) + Bu(t), \\ z(0) &= z_0, \end{aligned}\right\} \tag{4.2.50}$$

where $\tilde{A}$ and B are defined below. Let A be the differential operator

$$[A\phi](x) = \epsilon \frac{d^2\phi}{dx^2}(x), \tag{4.2.51}$$

defined on the domain $\mathcal{D}(A) \equiv H_0^1(0,1) \cap H^2(0,1)$, and let D denote the Dirichlet map $D : \mathbb{R}^2 \to L^2(0,1)$ given by

$$[Du](x) = (1-x)u_0 + xu_1. \tag{4.2.52}$$

The operator $\tilde{A} : L^2(0,1) \to [\mathcal{D}(A^*)]'$ is the lifting of A to $L^2(0,1)$ defined by

$$[\tilde{A}f](\psi) = \langle f, A^*\psi \rangle = \epsilon \int_0^1 f(x)\psi''(x)dx, \tag{4.2.53}$$

for each $\psi \in \mathcal{D}(A^*) = H_0^1(0,1) \cap H^2(0,1)$. Finally, the input operator $B : \mathbb{R}^2 \to [\mathcal{D}(A^*)]'$ is given by

$$B = -\tilde{A}D. \tag{4.2.54}$$

The adjoint of B is usually easier to represent than the operator itself; moreover, it is the adjoint that one needs in finite element approximations. In particular, one has

$$\begin{aligned}
\langle Bu, \phi \rangle &= -\langle Du, A^*\phi \rangle \\
&= -\epsilon \int_0^1 [(1-x)u_0 + xu_1]\phi''(x)dx \\
&= -\epsilon[(1-x)u_0 + xu_1]\phi'(x)\big|_0^1 + \epsilon(u_1 - u_0)\int_0^1 \phi'(x)dx \\
&= -\epsilon u_1 \frac{d\phi}{dx}(1) + \epsilon G u_0 \frac{d\phi}{dx}(0) \\
&= \langle u, B^*\phi \rangle_{\mathbb{R}^2}.
\end{aligned}$$

Hence, $B^* : \mathcal{D}(A^*) \to \mathbb{R}^2$ is given by $B^*\phi = \epsilon[\phi'(0), \ -\phi'(1)]^T$.

We consider a weighted LQR control problem defined by minimizing the cost function

$$J(u(\cdot)) \ = \ \int_0^\infty \{\langle y(t), y(t)\rangle + \langle u(t), u(t)\rangle\} \, e^{2\alpha t} dt \tag{4.2.55}$$

subject to the constraint (4.2.50), where $y(t) = Cz(t)$ is a controlled output function. It is well known (under suitable conditions on C) that the optimal control for this problem is given by feedback of the form

$$u(t) \ = \ Kz(t) \ = \ -B^*\Pi z(t), \tag{4.2.56}$$

where K is a feedback gain operator. Here, Π is the (weak) solution to the algebraic Riccati equation (ARE)

$$(\tilde{A} + \alpha I)^*\Pi + \Pi(\tilde{A} + \alpha I) - \Pi B B^* \Pi + Q \ = \ 0, \tag{4.2.57}$$

and $Q = C^*C$.

It is possible to show that the feedback operator K maps $L^2(0,1)$ to $\mathbb{R}^2$ and has the form

$$K\phi \ = \ \int_0^1 h(\xi)\phi(\xi)d\xi, \tag{4.2.58}$$

where the kernel $h(\cdot)$ belongs to $L^2(0,1)$. This kernel is called the functional gain and is useful in many applications. In previous research, Burns and Rubio use functional gains to optimally place sensors. Similar ideas have been used to construct low-order observers. A first step in both applications is the development of fast and accurate numerical schemes for computing $h(\cdot)$. This is the central theme of this work.

4.2.2 Riccati Methods

Conceptually, there are several ways to compute the functional gain. One basic approach is to approximate the ARE (4.2.57) and obtain an approximate Riccati operator Π^N. The approximate feedback operator is given by

$$K^N \ = \ -[B^*]^N \Pi^N, \tag{4.2.59}$$

and this feedback law yields an approximation $h^N(\cdot)$ to the functional gain $h(\cdot)$.

A more direct approach is to first obtain a representation for the Riccati operator of the form

$$[\Pi\phi](x) \ = \ \int_0^1 p(x,\xi)\phi(\xi)d\xi, \tag{4.2.60}$$

and to then solve for $p(x,\xi)$. For certain systems (distributed control and Neumann boundary control), Lions uses the Schwartz Kernel Theorem to obtain a representation of the form (4.2.60). Lions' result does not apply directly to the Dirichlet boundary control problem. However, King extended this result to the one-dimensional case considered here.

Theorem 4.2.1. *Assume $Q : L^2(0,1) \to L^2(0,1)$ is bounded. If $\Pi = \Pi^*$ is the unique, nonnegative-definite solution to the ARE (4.2.57), then Π is Hilbert-Schmidt. Moreover, there exists a function $p(x,\xi)$ such that Π has the representation (4.2.60) where the kernel $p(x,\xi)$ satisfies the condition:*

$$p(x,\xi) = p(\xi,x) \ \in \ C^1([0,1]\times[0,1]). \tag{4.2.61}$$

In order to apply this result, we assume that $C : L^2(0,1) \to \mathbb{R}$ has the form

$$C\phi(\cdot) \ = \ \int_0^1 c(x)\phi(x)dx, \tag{4.2.62}$$

where $c(x) \in L^2(0,1)$. Note that the operator $Q = C^*C$ has the form

$$\begin{aligned} [Q\phi](x) \ &= \ c(x)\int_0^1 c(\xi)\phi(\xi)d\xi \\ &= \ \int_0^1 q(x,\xi)\phi(\xi)d\xi, \end{aligned}$$

where $q(x,\xi)$ is the kernel for Q.

The following theorem extends the results in Lions to the Dirichlet boundary control problem considered here.

Theorem 4.2.2. *The kernel $p(x,\xi)$ of the operator Π is a weak solution to the Riccati partial differential equation (R-PDE)*

$$\begin{aligned} (A_x + A_\xi + 2\alpha I)p(x,\xi) - \frac{\partial}{\partial x}p(0,\xi)\frac{\partial}{\partial \xi}p(x,0) \\ + \frac{\partial}{\partial x}p(1,\xi)\frac{\partial}{\partial \xi}p(x,1) + q(x,\xi) \ = \ 0. \end{aligned} \tag{4.2.63}$$

In particular, $p(\cdot,\cdot) \in H_0^1([0,1]\times[0,1])$ satisfies the boundary conditions

$$\left.\begin{aligned} p(0,\xi) \ &= \ p(1,\xi) \ = \ 0, \quad \textit{and} \\ p(x,0) \ &= \ p(x,1) \ = \ 0, \end{aligned}\right\} \tag{4.2.64}$$

and the symmetry condition

$$p(x,\xi) \ = \ p(\xi,x), \quad \forall\ x,\xi \in (0,1). \tag{4.2.65}$$

Proof. The proof follows the same basic idea used by Lions for the case of distributed control with zero Dirichlet boundary conditions. Property (4.2.65) follows from $\Pi^* = \Pi$; that is,

$$[\Pi\phi](x) \ = \ \int_0^1 p(x,\xi)\phi(\xi)d\xi \ = \ \int_0^1 p(\xi,x)\phi(\xi)d\xi \ = \ [\Pi^*\phi](x).$$

From Theorem 3.1, $p(\cdot,\cdot)$ is in $C^1([0,1]\times[0,1])$. Suppose that, without loss of generality, $p(0,\xi_0) > 0$ for some fixed value of $\xi_0 \in (0,1)$. Since $p(0,\cdot) \in C^1(0,1)$, there exists a neighborhood $N_0 \subset (0,1)$ containing ξ_0 such that $p(0,\xi) > 0$ for all $\xi \in N_0$. It follows that $\Pi\phi \in \mathcal{D}(A)$ and hence $[\Pi\phi](0) = 0$ for all $\phi \in L^2(0,1)$. If $\phi(x) = 1$ on N_0 and $\phi(x) = 0$ elsewhere, then

$$[\Pi\phi](0) \ = \ \int_0^1 p(0,\xi)\phi(\xi)d\xi \ = \ \int_{N_0} p(0,\xi)d\xi \ \neq \ 0,$$

which contradicts the equality $[\Pi\phi](0) = 0$. Therefore, $p(0,\xi) = 0$ for all $\xi \in (0,1)$. The other boundary conditions in (4.2.64) are established by using analogous arguments.

To obtain (4.2.63), we substitute the representation of the Riccati operator into (4.2.57). Recall that the weak form of the ARE (4.2.57) is defined by

$$\langle \Pi\phi, A^*\psi\rangle + \langle A^*\phi, \Pi\psi\rangle + 2\alpha\langle \Pi\phi,\psi\rangle - \langle B^*\Pi\phi, B^*\Pi\psi\rangle + \langle C\phi, C\psi\rangle \;=\; 0, \tag{4.2.66}$$

for each $\phi, \psi \in \mathcal{D}(A)$. In particular, the first term in (4.2.66) is given by

$$\begin{aligned}\langle \Pi\phi, A^*\psi\rangle &= \int_0^1 \left[\int_0^1 p(x,\xi)\phi(\xi)d\xi\right]\psi''(x)dx \\ &= -\int_0^1\int_0^1 \frac{\partial}{\partial x}p(x,\xi)\psi'(x)\phi(\xi)dxd\xi.\end{aligned}$$

Let $V = H_0^1([0,1]\times[0,1])$ and define $A_x : V \to V^*$, by

$$[A_x p(x,\xi)](v(\cdot,\cdot)) \;=\; -\int_0^1\int_0^1 \frac{\partial}{\partial x}p(x,\xi)\frac{\partial}{\partial x}v(x,\xi)dxd\xi.$$

The operator A_ξ is defined similarly. The term $\langle C\phi, C\psi\rangle$ takes the form

$$\begin{aligned}\langle C^*C\phi,\psi\rangle &= \langle Q\phi,\psi\rangle \\ &= \int_0^1\left[\int_0^1 q(x,\xi)\phi(\xi)d\xi\right]\psi(x)dx \\ &= \int_0^1\int_0^1 q(x,\xi)\phi(\xi)\psi(x)dxd\xi.\end{aligned}$$

Finally, since $p(\cdot,\cdot)\in C^1([0,1]\times[0,1])$, it follows that

$$\begin{aligned}\langle \Pi BB^*\Pi\phi,\psi\rangle &= \langle B^*\Pi\phi, B^*\Pi^*\psi\rangle_{\mathbb{R}^2} \\ &= \left[B^*\textstyle\int_0^1 p(x,\xi)\phi(\xi)d\xi\right]^T\left[B^*\int_0^1 p(x,\xi)\psi(x)dx\right] \\ &= \textstyle\int_0^1\int_0^1\Big[\frac{\partial}{\partial x}p(0,\xi)\frac{\partial}{\partial\xi}p(x,0) \\ &\qquad +\frac{\partial}{\partial x}p(1,\xi)\frac{\partial}{\partial\xi}(x,1)\Big]\phi(\xi)\psi(x)dxd\xi.\end{aligned}$$

Therefore, $p(\cdot,\cdot)\in V = H_0^1([0,1]\times[0,1])$ satisfies the variational problem: Find $p(\cdot,\cdot)\in V$ such that for all $v(\cdot,\cdot)\in V$

$$\begin{aligned}&-\int_0^1\int_0^1\frac{\partial}{\partial x}p(x,\xi)\frac{\partial}{\partial x}v(x,\xi)dxd\xi - \int_0^1\int_0^1\frac{\partial}{\partial\xi}p(x,\xi)\frac{\partial}{\partial\xi}v(x,\xi)dxd\xi \\ &\quad + 2\alpha\int_0^1\int_0^1 p(x,\xi)v(x,\xi)dxd\xi \\ &\quad - \int_0^1\int_0^1\left[\frac{dp}{d\zeta}(0,\xi)\frac{dp}{d\zeta}(x,0) + \frac{dp}{d\zeta}(1,\xi)\frac{dp}{d\zeta}(x,1)\right]v(x,\xi)dxd\xi \\ &\quad + \int_0^1 q(x,\xi)v(x,\xi) \;=\; 0.\end{aligned} \tag{4.2.67}$$

Thus, the kernel $p(x,\xi)$ is a weak solution to (4.2.57). □

The feedback gain operator has the form

$$\begin{aligned}K\phi &= -B^*\Pi\phi \\ &= -B^*\left(\int_0^1 p(x,\xi)\phi(\xi)d\xi\right).\end{aligned}$$

Moreover, it has been shown that B^* can be moved inside the integral so that

$$K\phi \;=\; \int_0^1 -[B_x^* p](x,\xi)\phi(\xi)d\xi.$$

Thus, the functional gain $h(\xi)$ is given by

$$h(\xi) = -[B_x^* p](x,\xi) = [\ \partial p(0,\xi)/\partial x, \quad -\partial p(1,\xi)/\partial x\ ]^T.$$

4.2.3 Chandrasekhar Methods

Chandrasekhar methods have been used to bypass the step of solving for the Riccati operator. Formally, the Chandrasekhar equations are defined by

$$\left.\begin{aligned} \dot{K}(t) &= B^* L^*(t) L(t), \\ \dot{L}(t) &= -L(t)[\tilde{A} + \alpha I - BK(t)], \end{aligned}\right\} \tag{4.2.68}$$

with initial conditions

$$K(T) \;=\; 0 \qquad \text{and} \qquad L(T) \;=\; C. \tag{4.2.69}$$

Chandrasekhar equations have been applied to a number of distributed parameter systems. Under suitable conditions, one can show that $K(t) \to K$ as $t \to -\infty$. For the problem considered here, the Riesz Representation Theorem yields a functional gain $h(\cdot)$ so that

$$[K\phi] \;=\; \int_0^1 h(x)\phi(x)dx. \tag{4.2.70}$$

One can discretize the Chandrasekhar equations in the same manner as the discretization of the Riccati equations. In particular, one can construct approximations of the system and solve the corresponding ordinary differential equations

$$\left.\begin{aligned} \dot{K}^N(t) &= [B^*]^N [L^*]^N(t) L^N(t), \\ \dot{L}^N(t) &= -L^N(t)[\tilde{A}^N + \alpha I - B^N K^N(t)], \end{aligned}\right\} \tag{CE^N}$$

with initial conditions

$$K^N(T) \;=\; 0 \qquad \text{and} \qquad L^N(T) \;=\; C^N. \tag{4.2.71}$$

This approach has been used by a number of researchers. However, one loses spatial information that can be helpful in developing adaptive finite element methods for direct computation of $h(\cdot)$. A second approach is to derive the Chandrasekhar partial differential equations similar in spirit to the Riccati partial differential equation (4.2.63).

One formulates this system of partial differential equations for the functional gain by first assuming representations of the operators in the Chandrasekhar equations (4.2.68) and then proving the existence of these kernels. In particular, we seek kernels $h(t,\xi)$ and $l(t,\xi)$ such that

$$K(t)\phi \;=\; \int_0^1 h(t,\xi)\phi(\xi)d\xi \tag{4.2.72}$$

and

$$L(t)\phi \;=\; \int_0^1 l(t,\xi)\phi(\xi)d\xi, \tag{4.2.73}$$

respectively.

The kernels $h(\cdot,\cdot)$ and $l(\cdot,\cdot)$ satisfy the following Chandrasekhar partial differential equations (C-PDE)

$$\left.\begin{aligned} \tfrac{\partial h}{\partial t}(t,\xi) &= l(t,\xi)[B^*l](t,\xi), \\ \tfrac{\partial l}{\partial t}(t,\xi) &= -[(A+\alpha I)l](t,\xi) + h(t,\xi)[B^*l](t,\xi), \end{aligned}\right\} \tag{4.2.74}$$

with initial conditions

$$h(T,x) = 0 \quad \text{and} \quad l(T,x) = c(x), \tag{4.2.75}$$

where $c(x)$ is the kernel of the operator C. Also, $h(\cdot,\cdot)$ and $l(\cdot,\cdot)$ satisfy the boundary conditions

$$h(t,0) = h(t,1) = 0 \tag{4.2.76}$$

and

$$l(t,0) = l(t,1) = 0, \tag{4.2.77}$$

respectively.

Note that the term B^*l produced a boundary value so that (4.2.74)-(4.2.77) is a rather complex boundary value problem. In particular, the boundary terms B^* acting on the kernel $l(t,\cdot)$ yields

$$[B^*l](t,\xi) = \left[\frac{\partial}{\partial\xi}l(t,0), \quad -\frac{\partial}{\partial\xi}l(t,1)\right]^T.$$

The direct method involves solving (4.2.74) for $h(t,\cdot)$ and $l(t,\cdot)$, and using the fact that as $t \to -\infty$, $h(t,\xi) \to h(\xi)$ (the desired functional gain). To complete this program, one needs to establish existence and regularity of $h(t,\xi)$ and $l(t,\xi)$. In order to limit the length of this paper we do not address these issues here.

4.2.4 Approximations

We compute the functional gains by applying several finite element schemes to both approaches discussed above. In one case, we approximate the system $(\tilde{A}^N, B^N, Q^N, R^N)$ and solve the finite dimensional Riccati and Chandrasekhar equations. We also present results for direct finite element approximation of the Chandrasekhar partial differential equations.

Once a finite element subspace is selected, the first approach is to build matrix representations of the operators of the system (4.2.50) with cost function (4.2.55). In particular, we obtain $A^N \approx A$, $B^N \approx B$, $C^N \approx C$ and $R^N = R = I$. These matrix representations yield approximate Riccati equations (or Chandrasekhar equations) which can be solved using an appropriate numerical algorithm. The approximate solution Π^N or K^N yields an approximation $h^N(\cdot)$ of $h(\cdot)$.

We consider three finite element methods, and all methods employ piecewise linear elements. It is important to review these methods because the three schemes differ only in the implementation of the boundary conditions.

Recall, the global basis functions are defined by the piecewise linear "hat" functions

$$h_i(x) = \begin{cases} (x - x_{i-1})/h, & x_{i-1} \le x < x_i \\ (x_{i+1} - x)/h, & x_i \le x \le x_{i+1} \\ 0, & \textit{otherwise}, \end{cases} \tag{4.2.78}$$

where $h = i/(N+1)$ for $i = 1, \ldots, N$, and $N+1$ is the number of subintervals of $(0,1)$. At $x = 0$ and $x = 1$, $h_0(x)$ and $h_{N+1}(x)$ are given by

$$h_0(x) = \begin{cases} (h - x)/h, & 0 \le x < h \\ 0, & \textit{otherwise}, \end{cases}$$

and

$$h_{N+1}(x) = \begin{cases} (x - x_N)/h, & x_N \leq x \leq 1 \\ 0, & otherwise, \end{cases}$$

respectively.

The first method is "standard finite elements." The second method was used by Burns and Kang in their study of Burgers' equation and uses all $N+2$ basis functions. The third method is based on Nitsche's approximation as discussed in Section 10.1 of Lasiecka and Triggiani.

The standard finite element method is the most commonly discussed scheme. We find the solution to the problem in the subspace $V_0^h \subseteq H_0^1(0,1)$, where V_0^h is the space spanned by $h_i(x)$, $i = 1, \ldots, N$.

In V_0^h, the matrix representation for A is $A_0^N = (M_0^N)^{-1} S_0^N$ where M_0^N and S_0^N are the mass matrix and stiffness matrix, respectively. These matrices are given by

$$M_0^N = \frac{h}{6}\begin{bmatrix} 4 & 1 & 0 & \cdots & 0 \\ 1 & 4 & 1 & \cdots & 0 \\ 0 & 1 & 4 & \cdots & 0 \\ \vdots & & \vdots & \ddots & \vdots \\ 0 & 0 & 0 & \cdots & 4 \end{bmatrix}, \qquad S_0^N = \frac{\epsilon}{h}\begin{bmatrix} -2 & 1 & 0 & \cdots & 0 \\ 1 & -2 & 1 & \cdots & 0 \\ 0 & 1 & -2 & \cdots & 0 \\ \vdots & & \vdots & \ddots & \vdots \\ 0 & 0 & 0 & \cdots & -2 \end{bmatrix}.$$

The approximation B_0^N has the representation $(M^N)^{-1}\tilde{B}_0^N$ where

$$\tilde{B}_0^N = \frac{\epsilon}{h}\begin{bmatrix} 1 & 0 \\ 0 & 0 \\ \vdots & \vdots \\ 0 & 0 \\ 0 & 1 \end{bmatrix}. \tag{4.2.79}$$

The remaining finite element schemes attempt to adjust for the fact that the solutions are not zero on the boundaries. Bramble, et. al., consider these kinds of subspaces because they give optimal convergence rates for nonhomogeneous boundary conditions. Burns and Kang employ all $N+2$ basis functions and hence project the problem onto the space V^h spanned by $h_i(x)$, $i = 0, 1, \ldots, N+1$.

The resulting matrix representations for A^N and B^N are of size $(N+2) \times (N+2)$ and $(N+2) \times 2$, respectively. Thus, A^N has the representation $(M^N)^{-1}S^N$ and B^N has the representation $(M^N)^{-1}\tilde{B}^N$ where

$$M^N = \frac{h}{6}\begin{bmatrix} 2 & 1 & 0 & \cdots & 0 \\ 1 & 4 & 1 & \cdots & 0 \\ 0 & 1 & 4 & \cdots & 0 \\ \vdots & & \vdots & \ddots & \vdots \\ 0 & 0 & 0 & \cdots & 2 \end{bmatrix}, \qquad S^N = \frac{\epsilon}{h}\begin{bmatrix} -1 & 0 & 0 & \cdots & 0 \\ 1 & -2 & 1 & \cdots & 0 \\ 0 & 1 & -2 & \cdots & 0 \\ \vdots & & \vdots & \ddots & \vdots \\ 0 & 0 & 0 & \cdots & -1 \end{bmatrix}$$

and $\tilde{B}^N$ is the $(N+2) \times 2$ analog of (4.2.79).

Lasiecka and Triggiani suggested that Nitsche's approximation would be useful in the LQR problem because of improved accuracy of the Dirichlet boundary conditions. This scheme produces optimal convergence rates in the solution of the open-loop system. As we shall see below, the Nitsche scheme produces excellent approximations to the functional gains. The Nitsche method begins with the finite element scheme used by Burns and Kang. Nitsche's approximation A_β^N of the A operator is defined by

$$\langle A_\beta^N z^N, \phi^N \rangle = a(z^N, \phi^N) - \langle \frac{d}{dx} z^N, \phi^N \rangle_\Gamma - \langle z^N, \frac{d}{dx}\phi^N \rangle_\Gamma - \beta h^{-1} \langle z^N, \phi^N \rangle_\Gamma, \tag{4.2.80}$$

where $\beta > 0$ is sufficiently large, Γ is the boundary of the domain and $a(\cdot,\cdot)$ is the bilinear form such that

$$a(\phi,\psi) \;=\; -\int_0^1 \phi'(x)\psi'(x)dx.$$

Rearranging the terms of Nitsche's approximation A_β^N and using the fact that $z^N(0) = u_0$ and $z^N(1) = u_1$, the only matrices that are changed are the stiffness and the control matrices. The resulting stiffness matrix is the $(N+2)\times(N+2)$ matrix

$$S_\beta^N \;=\; \frac{\epsilon}{h}\begin{bmatrix} -1-\beta & 0 & 0 & \cdots & 0 \\ 1 & -2 & 1 & \cdots & 0 \\ 0 & 1 & -2 & \cdots & 0 \\ \vdots & & \vdots & \ddots & \vdots \\ 0 & 0 & 0 & \cdots & -1-\beta \end{bmatrix}, \tag{4.2.81}$$

and the control matrix is given by

$$\tilde{B}_\beta^N \;=\; \frac{\epsilon}{h}\begin{bmatrix} 1+\beta & 0 \\ 0 & 0 \\ \vdots & \vdots \\ 0 & 0 \\ 0 & 1+\beta \end{bmatrix}. \tag{4.2.82}$$

Again, Q is approximated by projecting onto V^h producing the approximate ARE defined by

$$(A^N+\alpha I^N)^*\Pi^N + \Pi^N(A^N+\alpha I^N) - \Pi^N B^N(B^N)^*\Pi^N + Q^N \;=\; 0, \tag{4.2.83}$$

It is clear that one can generate finite element approximations to the Riccati and Chandrasekhar partial differential equations by projecting these systems onto the various finite element spaces. In order to conserve space, we focus on the Chandrasekhar PDE (4.2.74)-(4.2.77). We turn now to numerical results that compare the schemes and methods mentioned in this section.

4.2.5 Numerical Results

In this section we present numerical comparisons for the methods described above. Two examples are presented. The first example compares the results obtained by applying the indirect method. We approximate the functional gains using the three finite element schemes mentioned in the previous section via the approximate ARE (4.2.83).

The second example focuses on the Chandrasekhar PDE system. We compare the standard finite element scheme with Nitsche's method. In particular, we use the standard finite element scheme to solve the Chandrasekhar PDE's (4.2.74)-(4.2.77), and compare this result to the Nitsche solution of the ARE (4.2.57).

Example 1. In this example, we take $Q = I$ in (4.2.55), and set $\epsilon = 1/60$, $\alpha = 0.3$. Figures 4.2.10 and 4.2.11 show plots of the approximate functional gains for all three methods. Figure 4.2.10 corresponds to control at $x = 0$ and Figure 4.2.11 contains plots for the functional gains for control at $x = 1$. Observe that at $N = 8$, the Nitsche scheme "corrects" the errors at the boundary that result from a direct application of the Burns-Kang scheme. The "converged" solution is represented by the $N = 128$ standard finite element solution. The closed-loop response is plotted in Figure 4.2.12. Figure 4.2.13 provides comparison of the closed-loop trajectories at time $t = 10$ seconds. Note that the Nitsche's scheme provides more accurate responses than the other methods. This observation has potential applications to controller reduction schemes.

Example 2. In this example, $c(x)$ is defined by

$$c(x) \;=\; \begin{cases} 0.5, & 0.6 \le x \le 0.8 \\ 0, & \textit{otherwise}, \end{cases}$$

and $\epsilon = 0.1$, $\alpha = 0$. The standard finite element scheme is applied to the Chandrasekhar PDE system (4.2.74)-(4.2.77). Nitsche's scheme is used to compute $h^N(x)$ via the ARE (4.2.83). Figures 4.2.14 and 4.2.15 show plots of the approximate functional gains for both schemes. The "converged" solution is represented by the same scheme used in the previous example. Note that both schemes produce excellent approximations to the functional gains. It is important to note that the convergence in space ($N \to \infty$) and time ($t \to -\infty$) of $h^N(t, \xi)$ to $h(\xi)$ is "fast enough" so that approximations of the Chandrasekhar PDE's are competitive with the other indirect approaches.

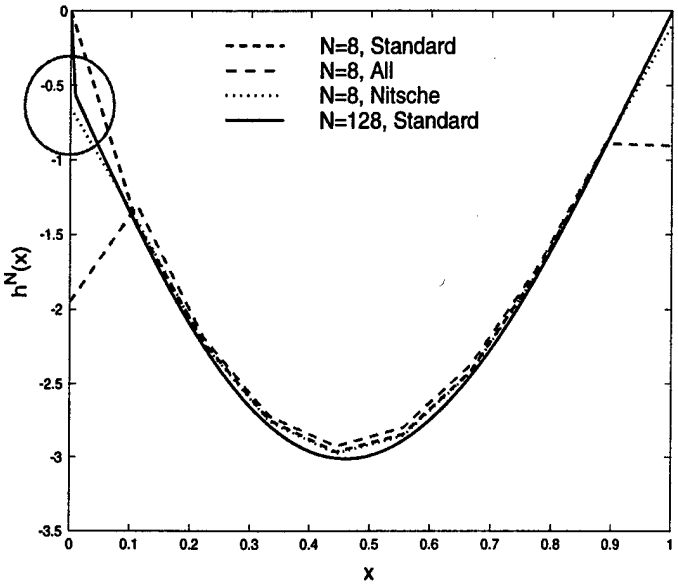

Figure 4.2.10: Functional Gain at $x = 0$, $N = 8$.

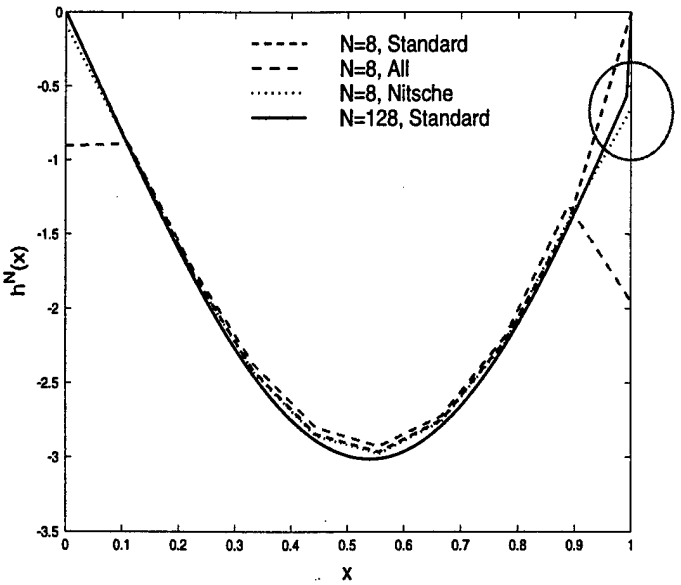

Figure 4.2.11: Functional Gain at $x = 1$, $N = 8$.

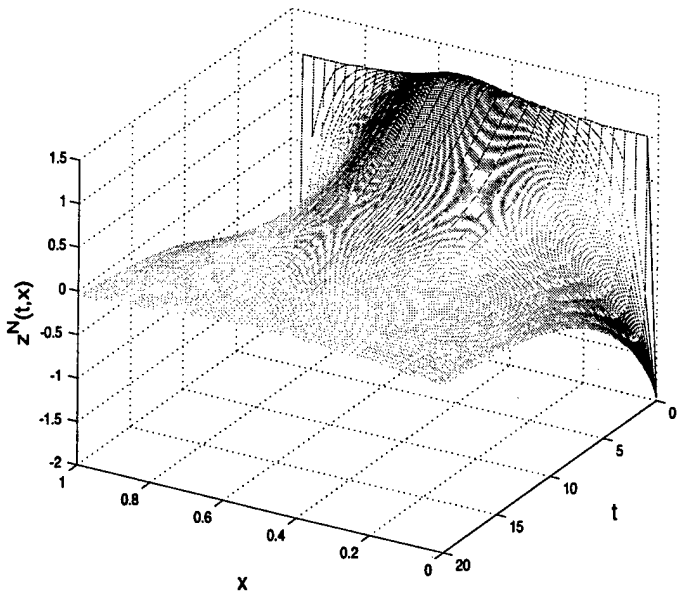

Figure 4.2.12: Solution of Closed-Loop System, $t = 0$ to $t = 20$.

4.2.6 Conclusion and Future Research

Although the numerical results presented here are not sufficient to provide conclusive information on the most efficient method for approximating functional gains, they do provide insight into these matters and they demonstrate the feasibility of the various schemes.

It is interesting to note that Nitsche's approximation produces excellent approximations to the functional gains. Hence, accuracy is improved by use of the Nitsche scheme. However, the Nitsche scheme was considerably slower than the standard finite element method. This was especially noticeable as N got larger. This is an issue that should be explored. In addition, the improved accuracy obtained by Nitsche's scheme was not uniform in N. In some cases, the standard finite element scheme was better at small N. Consequently, the tradeoffs between speed and accuracy are not yet settled.

Indirect methods (approximate first) have been useful in dealing with 1D and 2D problems. However, these indirect methods do not take advantage of the structure of the problem and do not allow for adaptive finite element refinements. The Riccati and Chandrasekhar PDE's offer the potential for improvements in these areas. These issues need to be explored.

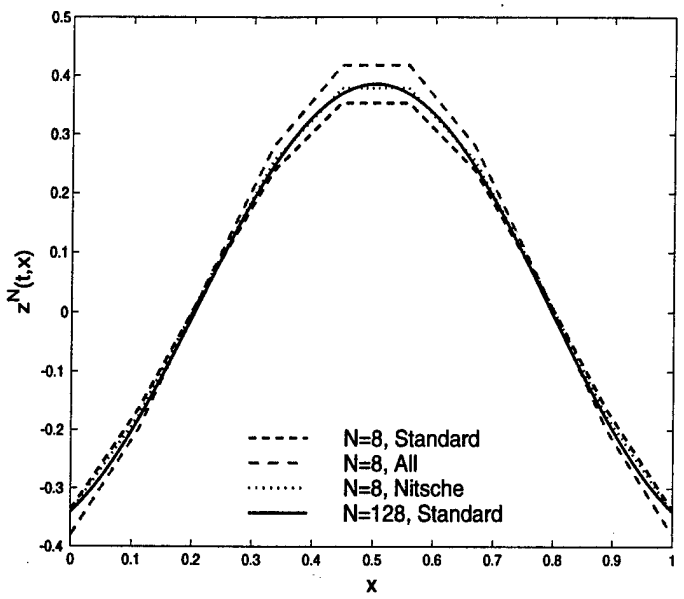

Figure 4.2.13: Closed-Loop Solution $z^8(t,x)$ at $t = 10.0$ sec.

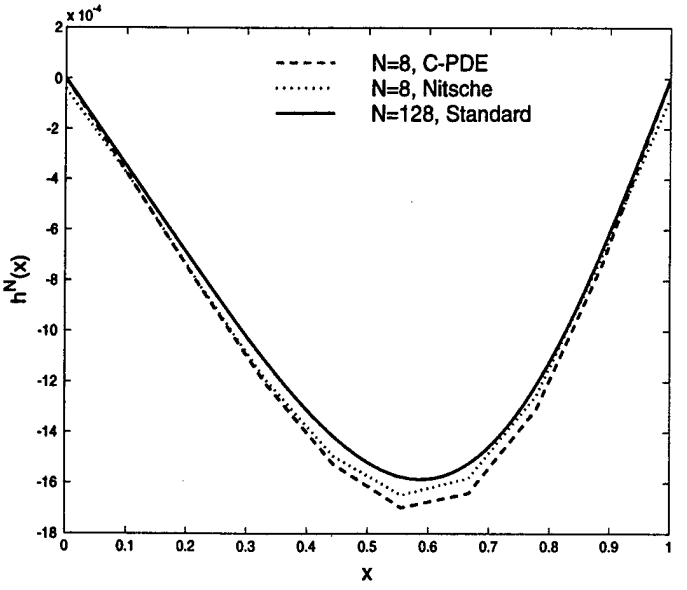

Figure 4.2.14: Functional Gain at $x = 0$, $N = 8$.

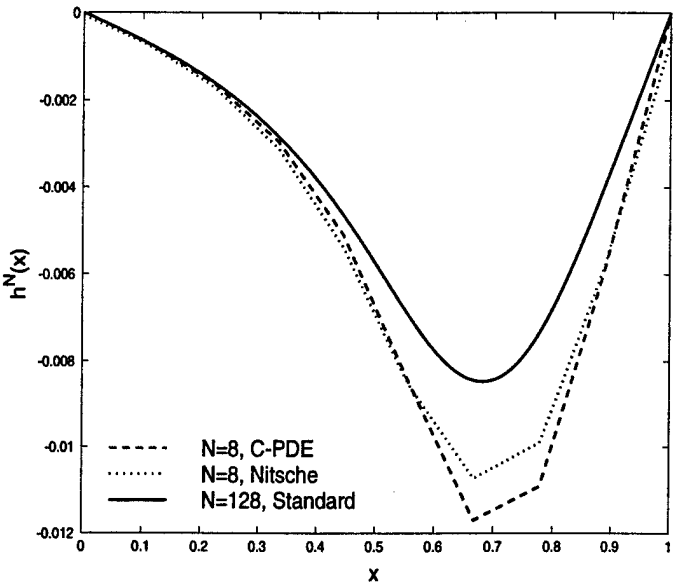

Figure 4.2.15: Functional Gain at $x = 1$, $N = 8$.

4.3 Significance and Potential Application to Air Force Problems

Hybrid Transformation Methods for Sensitivity Computations - Accurate sensitivity calculations play an important role in the analysis and optimization of engineering systems. Sensitivities can be used to compute gradients in optimization-based design. We focused on variational methods for computing state sensitivities. These schemes make use of sensitivity equation methods. However, there are a variety of ways to implement sensitivity equation methods, and these variations yield algorithms with different convergence properties. We considered two specific methods. The first is based on transforming the state equation to a fixed computational domain and then deriving its sensitivity equation. Once the state and sensitivity systems are solved, the solutions are mapped back to the physical domain. The second approach transforms both state and sensitivity equations, solves the transformed equations and maps these solutions back to the physical domain. There are benefits and drawbacks to each method. Indeed, it is not always obvious which scheme is best for a given problem. Many questions needed to be addressed before a complete theory could be developed.

Each of the methods present computational challenges. The Hybrid SEM requires gradient information along the boundary of the computational domain. This information becomes critical to accurate sensitivity calculations. However, other SEM often require accurate gradient information within the computational domain. This work clearly illustrated that serious contamination of sensitivity approximations can occur if the approximate spatial gradients are inaccurate or are not sufficiently smooth. Moreover, the Hybrid SEM avoids the need to calculate derivatives of mesh maps. In the case of the Hybrid method, accurate gradients is the only major stumbling block to obtaining reliable sensitivity calculations. In contrast, accurate gradient information may not be sufficient to obtain good sensitivity approximations using the other SAM methods, since the need for accurate mesh derivatives may overshadow the entire process. This work provided, for the first time, an understanding of the role that spatial smoothness plays in developing accurate numerical methods for sensitivity computations.

These results will play an important role in developing fast and accurate sensitivity analysis tools with Air Force applications such as wing-body design optimization, combustion control and COIL lasers.

Fast Algorithms for Computing Functional Gains - Functional gains are kernels of feedback operators that result from distributed parameter control problems defined by partial and functional differential equations. These gains offer insight into issues such as sensor/actuator placement and controller reduction. To be practical, one must be able to compute these kernels for a wide variety of partial differential equations in 2 and 3 spatial dimensions. Standard "approximate-then-design" approaches have been very useful for small 1D problems. However, in 2D and 3D problems, the size of the approximating systems limits this method as a practical computational tool. Therefore, alternative methods were needed.

As a first step in the direction we developed "direct" approximations of Riccati and Chandrasekhar partial differential equations that define these kernels. This direct approach allows for the possibility of using parallel and adaptive computational tools. In addition, we established that by modifying "standard" finite element schemes one can improve the speed and accuracy of the old indirect schemes. In particular, so called "Nitsche methods" produces greatly improved approximations to the functional gains. Although the standard Nitsche scheme improved accuracy, it was considerably slower than other finite element methods. This was especially noticeable as the number of elements grew. Riccati and Chandrasekhar PDE's offers the potential for improvements in this areas.

These methods have already proven to be useful in the control of 2D thermal processes and when extended to Navier-Stokes equations will provide the basic tools needed to accomplish practical sensor/actuator placement and controller reduction for flow control. In addition, these tools will be useful in several other DOD applications; including the design and control of materials manufacturing processes and control of combustion.

Chapter 5

Personnel Supported

The following people were supported in part under AFOSR *ASSERT* Grant F49620-97-1-0356 and/or associated with the research effort:

5.1 Faculty Associated with the Research Effort

- Jeff Borggaard
- John A. Burns
- Eugene M. Cliff
- Terry Herdman
- Belinda B. King

5.2 Graduate Students Supported

- Kevin Hulsing, Ph.D. 1999
- Lisa Stanley, Ph.D. 1999
- Dawn Stewart, Ph.D. 1998

Chapter 6

Publications

The following publications were produced during the funding period under AFOSR *ASSERT* Grant F49620-97-1-0356:

6.1 Publications by Students

1. Burns, J. A. and Hulsing, K.P., Numerical Methods for Approximating Functional gains in LQR Boundary Control Problems, *Mathematical and Computer Modelling*, accepted.

2. Burns, J.A., Stanley, L.G. and Stewart, D.L. A Projection Method for Accurate Computation of Design Sensitivities, *Optimal Control: Theory, Algorithms and Applications*, W. Hager and P. Pardalos, Eds., Kluwer Academic Publishers B.V., 1997, 40-66.

3. Burns, J. A. and Stanley, L.G, A Note on the Use of Transformations in Sensitivity Computations for Elliptic Systems, *Mathematical and Computer Modelling*, accepted.

4. Chen., H., Hatch, A., Peters, G., Pritchett, L., Stanley, L. and Scheprov, A. Pressure Tube Modeling Problem, in *1997 Industrial Mathematics Modeling Workshop for Graduate Students*, F. Reitich, J. Scroggs, and H. Tran, Eds., Raleigh, NC, 1998, 11-25.

5. Gablonsky, J., Hulsing, K., McShine, L., Pihlaja, A., Seshaiyer, P. and Settumba, N. Sipe Consolidation in Tire Design, in *1997 Industrial Mathematics Modeling Workshop for Graduate Students*, F. Reitich, J. Scroggs, and H. Tran, Eds., Raleigh, NC, February 1998, 26-35.

6. Stanley, L.G. and Stewart, D.L. A Comparison of Local and Global Projections, in *Design Sensitivity Computations in Proceedings of the 1997 AFOSR Workshop on Optimal Design and Control*, J. Borggaard, J. Burns, E. Cliff, and S. Schreck, Eds., Birkhauser, 1998, 59-76.

7. Stewart, D. L., Numerical Methods for Accurate Computation of Design Sensitivities for Two-Dimensional Navier-Stokes problems, submitted.

6.2 Publications by Principle Investigator

1. Balogh, A., Burns, J., Gilliam, D. and Shubov, V., A Note on Numerical Stationary Solutions for the Viscous Burgers' Equation, *Journal of Math. Systems, Estimation, and Control*, Vol. 8, No. 2, (1998), 253-256. Full electronic manuscript published March, 1998, 16 pp. Retrieval code: 55578.

2. Borggaard, J. and Burns, J., A PDE Sensitivity Equation Method for Optimal Aerodynamic Design, *Journal of Computational Physics*, Vol. 136, (1997), 366-384.

3. Borggaard, J. and Burns, J., Asymptotically Consistent Gradients in Optimal Design, *Multidisciplinary Design Optimization*, N. M. Alexandrov and M. Y. Hussaini, Ed., SIAM Publications, 1997, 303-314.

4. Burns, J., Kang, S., Kachroo, P. and Ozbay, K., System Dynamics and Feedback Control Formulations for Real Time Dynamic Traffic Routing, *Journal of Mathematical and Computer Modeling*, Vol. 27, No. 9, (1998), 27-49.

5. Burns, J. and King, B., A Note on the Mathematical Modeling of Damped Second Order Systems, *Journal of Math. Systems, Estimation, and Control*, Vol. 8, No. 2, (1998), 189-192. Full electronic manuscript published March, 1998, 12 pp. Retrieval code: 82674.

6. Burns, J., King, B. and Rubio, D., Control of a Thermal Fluid Using State Estimators, *International Journal of Computational Fluid Dynamics*, Vol. 11, (1998), 393-112.

7. Burns, J. and Rubio, D., A Control Distributed Parameter Control Approach to Sensor Location for Optimal Feedback Control of Thermal Processes, *36th IEEE Conference on Decision and Control*, December 1997, 2243-2247.

8. Berger, S., Burns, J., Burr, R. and Gilmore, P., Automated Optimization Techniques for Phase Change Piezoelectric Ink Jet Performance Enhancement, *1997 International Conference on Digital Printing Technologies*, Society for Imaging Science and Technology, IS&T's NIP13, November, 1997, 716-721.

9. *Computational Methods for Optimal Design*, Edited by Jeff Borrggaard, John Burns, Eugene Cliff and Scott Schreck, Progress in Systems and Control Theory, Birkhäuser, Boston, 1998, 475 pages.

10. Burns, J., King, B. and Rubio, D., On the Design of Feedback Controllers for a Convecting Fluid Flow via Reduced Order Modeling, *1999 IEEE International Conference on Control Applications*, to appear.

Chapter 7

Interactions and Transitions

One of the major components of this effort is active cooperation and coordination with Air Force laboratories and with industrial partners. The *ASSERT* students are active participants in the *PRET* Center and frequently interact with our industrial partners. In addition, these students have been invited to present their research at national and international conferences.

7.1 Participation and Presentations at Meetings

Kevin Hulsing

1. *Sipe Consolidation in Tire Design*, Industrial Mathematics Modeling Workshop for Graduate Students, N.C. State University, Raleigh, NC, August 1997.
2. *Methods for Computing Feedback Operators for LQR Control*, University of Trier, Trier, Germany, February 1998.
3. *Methods for Computing Feedback Operators for LQR Control*, Fourth SIAM Conference on Control & Its Application, Jacksonville, FL, May 1998.
4. *Methods for Computing Feedback Operators for LQR Control*, Computation and Control VI, Montana State University, Bozeman, MT, August 1998.

Lisa Stanley

1. *Two Projection Methods for Approximating Derivatives of Computed Solutions to PDEs*, University of Trier, Trier, Germany, March 1998.
2. *Two Projection Methods for Approximating Derivatives of Computed Solutions to PDEs*, Fourth SIAM Conference on Control & Its Applications, Jacksonville, FL, May 1998.
3. *A Comparison of Two Methods for Computing Sensitivities*, Control and Computation VI, Montana State University, Bozeman, MT, August, 1998.
4. *A Comparison of Two Methods for Computing Sensitivities*, Sixth SIAM Conference on Optimization, Atlanta, GA, May 1999.
5. *Optimal Inverse Design using Sensitivity Analysis* ASME Mechanics and Materials Conference, Virginia Tech, Blacksburg, VA, June 1999.
6. *Transformation Techniques in Sensitivity Computations for Elliptic Systems*, Montana State University, Bozeman, MT, August 1999.

John Burns

1. *Reduced Order Compensator Design for Distributed Parameter Systems*, XX Congresso Nacional Matematica, Gramado, Brazil, September 1997.
2. *Sensitivity equation Methods for Optimal Design*, Conference on Multidisciplinary Design Optimization, Montreal, Quebec, March 1998.
3. *A Distributed Parameter Approach to Optimal Sensor Location and Controller Reduction*, DARPA Workshop on Materials Processing and Control, Washington, DC, April 1998.
4. *Hybrid Sensitivity Equation Methods with Application to Aerodynamic Design*, International Conference on Distributed Parameter Control, Hangzhou, China, June 1998.
5. *Optimization Based Design of PDE Systems*, Jiao Tong University, Shanghai, China, June 1998.
6. *Sensitivity Equation Methods for Optimal Design*, North Carolina State University, Raleigh, NC, December 1998.
7. *Computational Methods for Sensitivity Analysis in Optimal Design*, Texas Tech University, Lubbock, TX, February 1999.
8. *Sensitivitivies in Optimal Design*, International Conference on Optimization, Trier, Germany, March 1999.
9. *Optimal Control Approaches to Engineering Design: Numerical and Mathematical Issues*, Regional Meeting of the AMS, Las Vegas, NV, April 1999.

Chapter 8

Inventions and Patents

No patents nor trademarks were applied for during this period.

Chapter 9

Honors and Awards

None